

file

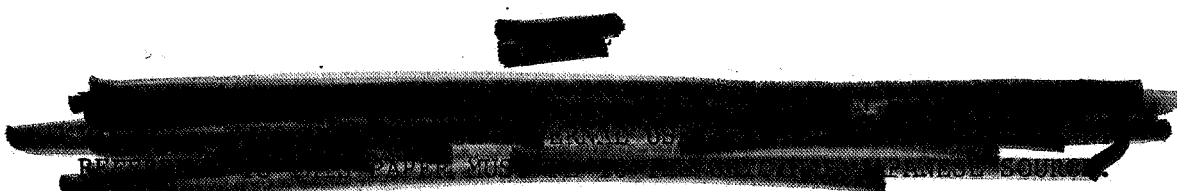
STUDIES ON THE MECHANICAL PROPERTIES OF FILAMENT-WOUND MATERIALS
AND METHODS USED IN THEIR MEASUREMENT (I)

THE DETERMINATION OF ELASTIC MODULI OF FILAMENT-WOUND CYLINDERS

Shinji Fukui, Kozo Kawata, Akira Kobayashi, and
Shozo Hashimoto

Translation of F/W FRP の力学特性と測定法について (I)

— F/W 円筒での弾性係数の決定 —

Bulletin of Tokyo University Space and Aeronautics
Research Institute, Vol. 2, No. 2, Apr. 1966

FACILITY FORM 602	N69-71941	
	(ACCESSION NUMBER)	(THRU)
	12	NONE
	(PAGES)	(CODE)
	✓	
	(NASA CR OR TMX OR AD NUMBER)	(CATEGORY)

NATIONAL AERONAUTICS AND SPACE ADMINISTRATION
WASHINGTON JANUARY 1967

STUDIES ON THE MECHANICAL PROPERTIES OF FILAMENT-WOUND MATERIALS
AND METHODS USED IN THEIR MEASUREMENT (I)
THE DETERMINATION OF ELASTIC MODULI OF FILAMENT-WOUND CYLINDERS

Shinji Fukui, Kozo Kawata, Akira Kobayashi, and
Shozo Hashimoto

ABSTRACT

As a part of studies on the mechanical properties of F/W materials, the methods of determining four elastic moduli, namely Young's moduli E_1 , E_2 , Poisson's ratios ν_1 and ν_2 of F/W cylinders as orthotropic plates were discussed (axial and circumferential directions were used as the principal directions 1 and 2 respectively); and a relationship between these values and the winding pattern was obtained. Considerable differences exist between the true E_1 and E_2 values and the apparent values. The possible upper limits of the F/W cylinder under internal pressure are also discussed.

1. Introduction

One of the aerospace materials is filament-wound (abbr. as F/W hereafter) /497* material, a type of FRP. This material is frequently used in a cylindrical or a similar form which is subjected to internal pressure, such as in a rocket chamber. Therefore, as a part of a series of studies on F/W materials which are to be continued in the future, a few studies were made on the mechanical properties of the materials in the above-mentioned forms and the methods used in their measurement.

Part I of the series is reported in this paper. This section concerns the determination of elastic moduli of F/W cylinders. F/W cylinders were used as is instead of in small specimens with broken fibers at the end, and attempts were made to determine four elastic constants (Young's moduli, E_1 , E_2 , Poisson's /498 ratios ν_1 and ν_2 with 1 and 2 as the principal directions) of the cylinders as orthotropic plates. Disregarding the changing appearance caused by winding pattern and ν_1 , ν_2 , it was proven that the apparent E_1 obtained from σ_1/ϵ_1 and the apparent E_2 obtained from σ_2/ϵ_2 differ a great deal from the true E_1 and E_2 .

2. Methods of Measuring the Plane Stress and the Elastic
Constant of Orthotropic Plates

Before deriving the methods of measurement, we would like to explain briefly

*Numbers given in the margin indicate the pagination in the original foreign text.

the stress-strain relationships in plane stress on orthotropic plates. F/W cylinders, when developed, can be considered as orthotropic plates. Generally, there are two elastic axes of symmetry (principal elastic directions), 1 and 2, of orthotropic plates, and the elastic law for these directions can be expressed in the same form as that for isotropic plates. In Figure 1, the symbols are as follows:

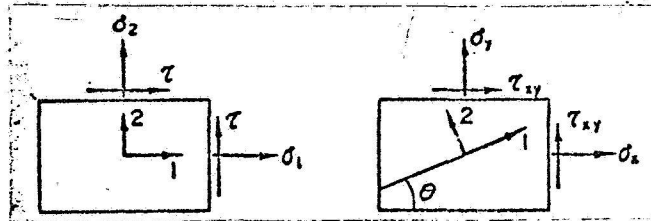


Fig. 1 Elastic law of principal elastic direction and general direction.

1, 2: principal elastic direction.

σ_1, σ_2, τ : Tensile stress σ in directions 1 and 2, and the shearing stress τ between them.

E_1, E_2 : Young's moduli of directions 1 and 2.

ν_1, ν_2 : Poisson's ratios to directions 1 and 2.

G : shearing elastic moduli between 1 and 2.

$\epsilon_1, \epsilon_2, \gamma$: elongation strain of directions 1 and 2, and shearing strain between 1 and 2.

x, y : orthogonal axes, forming angle θ and principal directions of elasticity 1 and 2.

$\sigma_x, \sigma_y, \tau_{xy}$: tensile stress to shearing stress in x, y directions.

strain components to the above stress components.

under these conditions:

$$\left. \begin{aligned} \epsilon_1 &= \frac{\sigma_1}{E_1} - \nu_2 \frac{\sigma_2}{E_2} \\ \epsilon_2 &= \frac{\sigma_2}{E_2} - \nu_1 \frac{\sigma_1}{E_1} \\ \gamma &= \frac{\tau}{G} \end{aligned} \right\} \quad (1)$$

Further, the following reciprocal relation is established:

$$\frac{\nu_1}{E_1} = \frac{\nu_2}{E_2} \quad (2)$$

As for the general directions,

$$\left. \begin{aligned} \epsilon_x &= l^2 \epsilon_1 + m^2 \epsilon_2 - lm \gamma \\ \epsilon_y &= m^2 \epsilon_1 + l^2 \epsilon_2 + lm \gamma \\ \gamma_{xy} &= 2 lm (\epsilon_1 - \epsilon_2) + (l^2 - m^2) \gamma \\ l &= \cos \theta, \quad m = \sin \theta \end{aligned} \right\} \quad (3)$$

$$\left. \begin{aligned} \sigma_1 &= l^2 \sigma_x + m^2 \sigma_y + 2 lm \tau_{xy} \\ \sigma_2 &= m^2 \sigma_x + l^2 \sigma_y - 2 lm \tau_{xy} \\ \tau &= -lm (\sigma_x - \sigma_y) + (l^2 - m^2) \tau_{xy} \end{aligned} \right\} \quad (4) \quad /499$$

$$\left. \begin{aligned} \epsilon_x &= \frac{\sigma_x}{E_x} + \frac{\sigma_y}{F} + \frac{\tau_{xy}}{H} \\ \epsilon_y &= \frac{\sigma_x}{F} + \frac{\sigma_y}{E_y} + \frac{\tau_{xy}}{K} \\ \tau_{xy} &= \frac{\sigma_x}{H} + \frac{\sigma_y}{K} + \frac{\tau_{xy}}{G_{xy}} \end{aligned} \right\} \quad (5)$$

$$\left. \begin{aligned} \frac{1}{E_x} &= \frac{l^4}{E_1} + \frac{m^4}{E_2} + l^2 m^2 \left(\frac{1}{G} - \frac{2\nu_1}{E_1} \right) \\ \frac{1}{E_y} &= \frac{m^4}{E_1} + \frac{l^4}{E_2} + l^2 m^2 \left(\frac{1}{G} - \frac{2\nu_1}{E_1} \right) \\ \frac{1}{G_{xy}} &= \frac{1}{G} + 4 l^2 m^2 \left(\frac{1}{E_1} + \frac{1}{E_2} + \frac{2\nu_1}{E_1} - \frac{1}{G} \right) \\ \frac{1}{F} &= -\frac{\nu_1}{E_1} + l^2 m^2 \left(\frac{1}{E_1} + \frac{1}{E_2} + \frac{2\nu_1}{E_1} - \frac{1}{G} \right) \\ \frac{1}{H} &= 2 l^3 m \left(\frac{1+\nu_1}{E_1} \right) - 2 lm^3 \left(\frac{1+\nu_2}{E_2} \right) - lm(l^2 - m^2) \frac{1}{G} \\ \frac{1}{K} &= 2 l^3 m \left(\frac{1+\nu_1}{E_1} \right) - 2 lm^3 \left(\frac{1+\nu_2}{E_2} \right) + lm(l^2 - m^2) \frac{1}{G} \end{aligned} \right\} \quad (6)$$

Five elastic constants appear here, namely E_1 , E_2 , ν_1 , ν_2 , and G , but there are four independent elastic constants because of the reciprocal relation (2). Consequently, in order to determine these, four independent relative equations are required.

3. Methods of Measurement

Since G is obtained by torsion experiments, it is handled separately here, and E_1 , E_2 , ν_1 , ν_2 are considered. In order to obtain these, $4 - 3 = 3$ independent relative equations are sufficient.

(1) Internal Pressure Test of Cylinder

Axial direction and circumferential direction of the cylinder are 1 and 2, respectively. We shall assume a situation in which numerous strain gauges are attached to the surface of the cylinder and the directions of the gauges are varied by angle θ , which is assumed to include both 0° and 90° . When $\theta = 0^\circ$ and 90° , we can compute σ_1 and σ_2 from the internal pressure, P , so that two independent relations can be obtained from equation (1): /500

$$\left. \begin{aligned} \epsilon_1 &= \frac{\sigma_1}{E_1} - \nu_1 \frac{\sigma_2}{E_2} \\ \epsilon_2 &= \frac{\sigma_2}{E_2} - \nu_2 \frac{\sigma_1}{E_1} \end{aligned} \right\}$$

(7)

and, as can be seen from equations (3) and (4), the relations E_x , E_y , σ_x , σ_y , for other θ do not yield independent relations and can only be used for checking the above data.

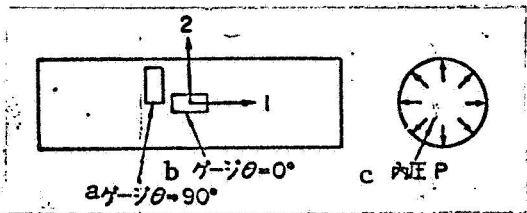


Fig. 2 Measurement in a cylinder under internal pressure.

Key:

- a. gauge angle $\theta = 90^\circ$
- b. gauge angle $\theta = 0^\circ$
- c. internal pressure P .

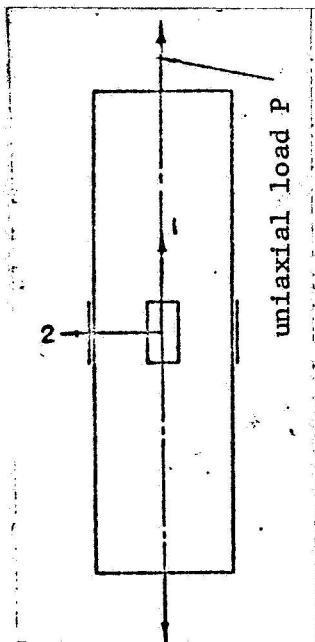


Fig. 3 Measurement in a cylinder subject to uniaxial load in the axial direction.

(2) Uniaxial Tension in Cylinder

When uniaxial tension is loaded as shown in Fig. 3,

$$\epsilon_1 = \frac{\sigma_1}{E_1} \quad \sigma_2 = 0 \quad (8)$$

From the above (7) and (8), the three necessary independent relative equations are obtained.

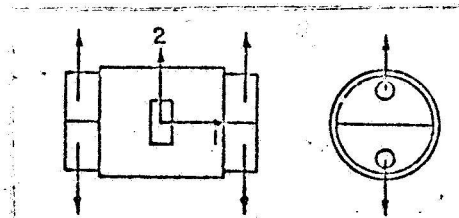


Fig. 4 Measurement with the ISAS ring test.

(3) ISAS Ring Test

This may be used for verifying E_2 .

When the above-mentioned equations (7) and (8) are used, first from (8),

$$E_1 = \frac{\sigma_{1(2)}}{\epsilon_{1(2)}} \quad (9)$$

is obtained; next, from (7),

$$\epsilon_{1(1)} = \frac{\sigma_{1(1)}}{E_1} - \nu_2 \frac{\sigma_{2(1)}}{E_2} = \frac{\sigma_{1(1)}}{E_1} - \nu_1 \frac{\sigma_{1(1)}}{E_1} \quad (10)$$

$$\nu_1 = \frac{1}{\sigma_{1(1)}} (\sigma_{1(1)} - \epsilon_{1(1)} E_1) \quad (11)$$

$$E_2 = \frac{\sigma_{2(1)}}{\epsilon_{2(1)} + \nu_1 / E_1 \sigma_{1(1)}} \quad (12)$$

$$\nu_2 = \frac{E_2 \nu_1}{E_1} \quad (12)$$

Subscripts (1) and (2) indicate respectively the values obtained from the internal pressure test and the uniaxial tension test of cylinders.

4. F/W Cylindrical Specimens

/501

The details of specimens are shown in Table 1 and Fig. 5.

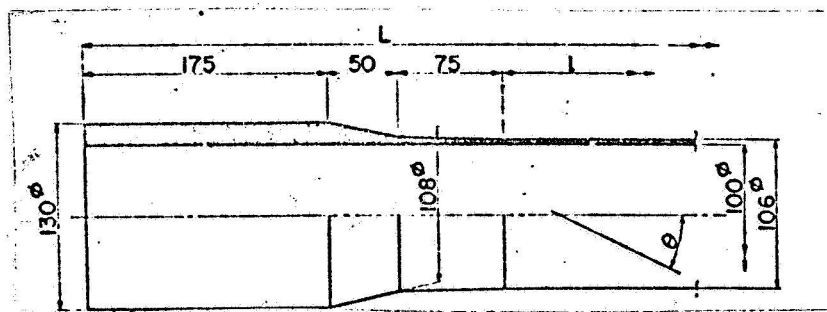


Fig. 5 Dimension of F/W cylindrical specimens.

Table 1. F/W Cylindrical Specimens

No.	Total length L(mm)	Parallel area l (mm)	Winding angle θ (deg)	Constitution**
1	650	50	40	spiral winding + circumferential winding
2	800	200	40	"
3	1000	400	40	"
4 103*	"	"	20	"
5 106*	"	"	50	"
6 107*	"	"	70	"
7 108*	"	"	40	spiral winding only

glass fiber roving 20 ends cross x ECE 20 230
 resin epoxy (*epicoat 828) curing agent HHPA

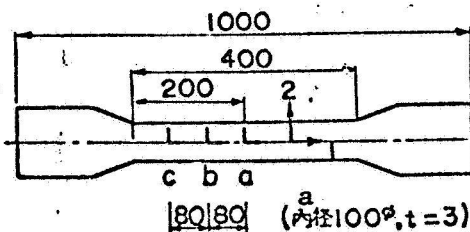
glass content, about 75% (wt.)

*Nos. in Figs. 7-10

**According to netting analyses, the fiber distributions in all cases are of equal values as one axial direction and two circumferential directions.

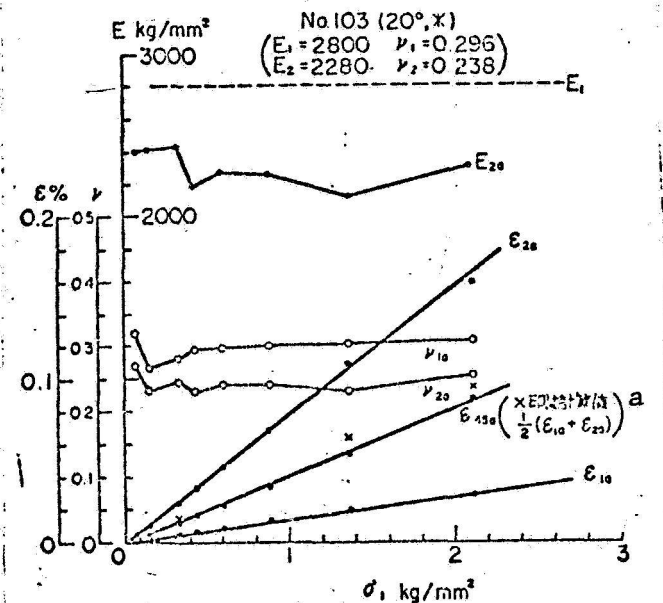
5. Results of Actual Measurements and their Evaluation, Upper Limits of E of the F/W Cylinder

The method of measurement was: first E_1 was obtained by uniaxial loading as described in 3, then data was obtained from internal pressure tests.



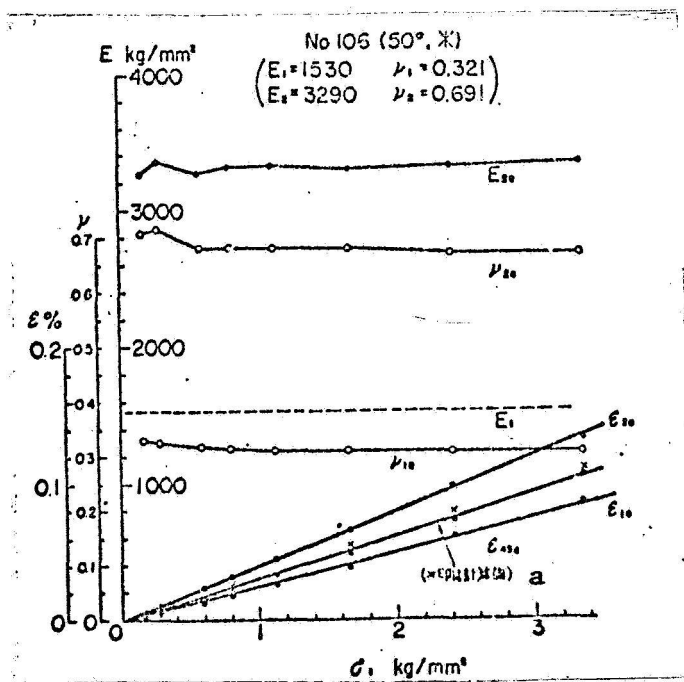
a = inner diameter

Fig. 6 Position for Strain Measurements.



$a = \text{sign X is the calculated value}$
 $\frac{1}{2}(\epsilon_{10} + \epsilon_{20})$

Fig. 7 Measurement of the elastic constant in cylindrical specimens with winding angles of 20° + 90°.



$a = (\text{sign X is the calculated value})$

Fig. 8 Measurement of the elastic constant in cylindrical specimens with winding angles of 50° + 90°.

The results of measurements by means of attaching an 8% strain gauge at the position shown in Fig. 6, were plotted against the principal axial stress σ_1 obtained in the internal pressure test. The results are shown in Figs. 7 - 10. The summarized results are as shown in Figs. 11 and 12. As seen in Figs. 7 - 10, the measured values of these constants scatter slightly where the stresses are very small, but show good conformity. The measured strain values of ϵ_{45} , in the direction where $\theta = 45^\circ$, agree well with the values calculated from ϵ_1 and ϵ_2 and prove the accuracy of the measurements. In Figs. 11 and 12, the specimen with a winding angle of 40° alone did not include winding in the circumferential direction ($\theta=0^\circ$), and the trend is off compared with those of the other three, but this is only natural. It should be noted that in Table 2, the differences between the true E_1 , E_2 and the apparent E_1 , E_2 (i.e., $\sigma_1(1)/\epsilon_1(1)$, $\sigma_2(1)/\epsilon_2(1)$) are quite pronounced. E_1 and E_2 in Table 2 range from 1000 kg/mm^2 to 4000 kg/mm^2 . However, we shall study the possible upper limit in the F/W cylinders having the fiber direction distributed most logically to see what point E_1 and E_2 can attain. Now, assuming a rocket chamber, the cylinder under internal pressure is $\sigma_2/\sigma_1 = 2$, therefore, it would be logical to set the distribution of fiber directions as two circumferential directions, and one axial direction, or a distribution having values equal to these. Therefore, disregarding polymers where E is very low compared with fibers, the possible upper limit of E in an FRP F/W cylinder under internal pressure is considered to be: longitudinal axial direction: $1/3 E_f$, circumferential direction: $2/3 E_f$ (E_f : Young's modulus for fibers). When E glass (E 7000 kg/mm^2) is taken as fibers, the values are around 2300 kg/mm^2 and 4600 kg/mm^2 , respectively.

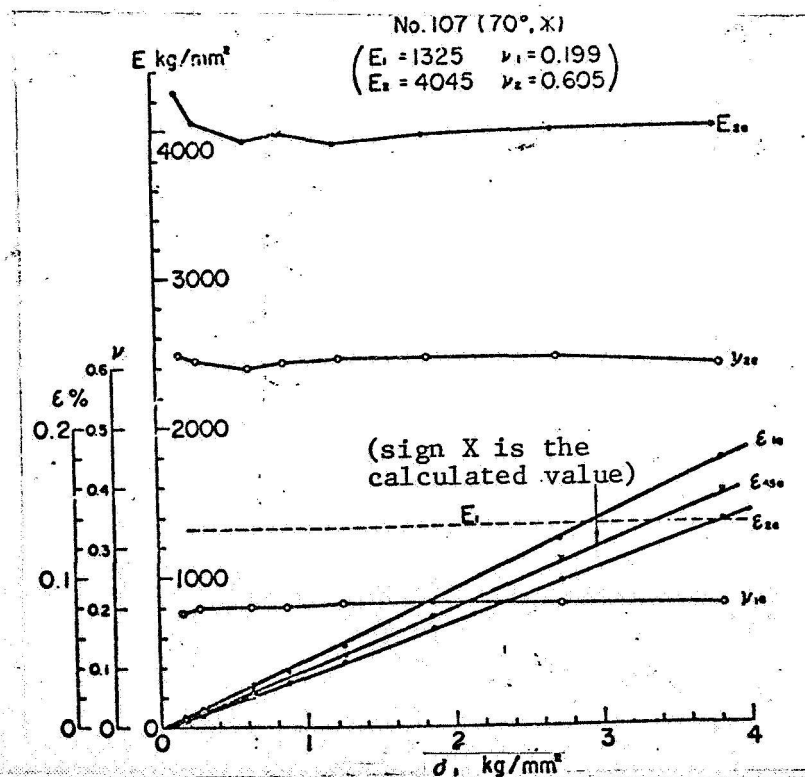


Fig. 9 Measurement of the elastic constant in cylindrical specimens with winding angles of $70^\circ + 90^\circ$.

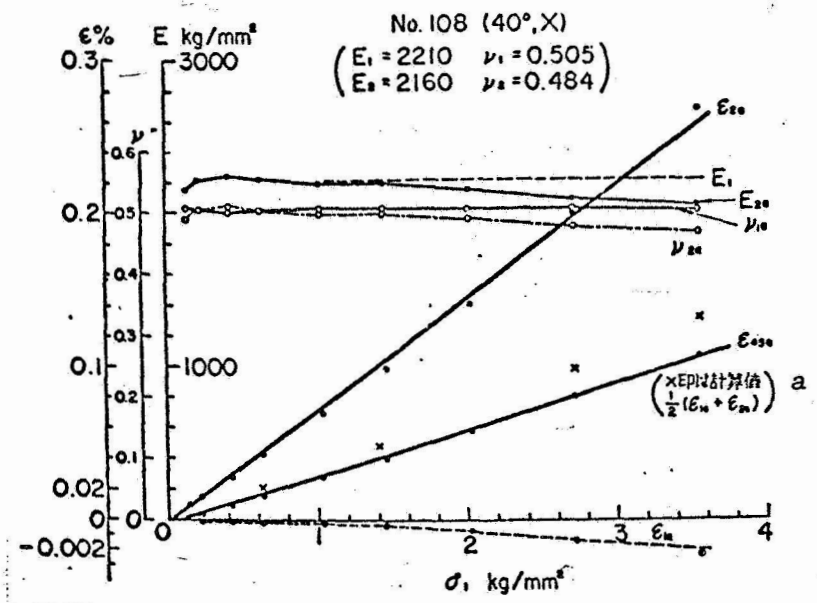


Fig. 10 Measurement of the elastic constant in cylindrical specimens with a winding angle of 40°.

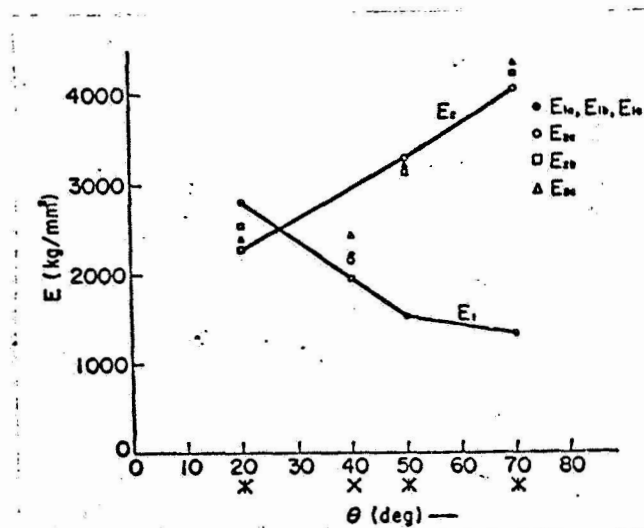


Fig. 11 Relationship of E_1 and E_2 to winding angles.

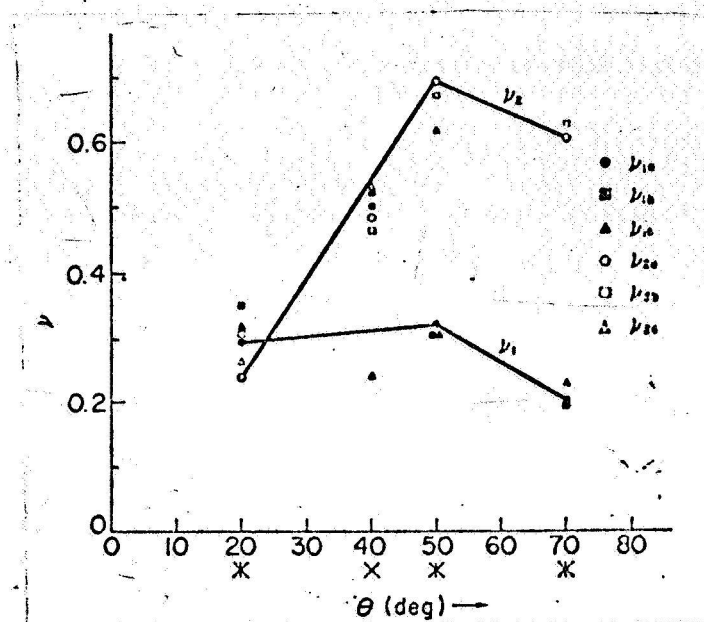


Fig. 12 Relationship of ν_1 and ν_2 to winding angles.

Table 2. True E_1 , E_2 , ν_1 , ν_2 and apparent E_1 , E_2 of F/W cylindrical specimens.

winding angle θ (deg)	$20^\circ+90^\circ$ *	40° x	$50^\circ+90^\circ$ *	$70^\circ+90^\circ$ *
E_1 (kg/mm ²)	2800	2210	1530	1325
$\frac{\sigma_{1(t)}}{\epsilon_{1(t)}} \text{ (kg/mm}^2\text{)}$	6790	- 290	4310	2380
E_2 (kg/mm ²)	2280	2160	3290	4045
$\frac{\sigma_{2(t)}}{\epsilon_{2(t)}} \text{ (kg/mm}^2\text{)}$	2620	2380	5030	5850
ν_1	0.296	0.505	0.321	0.199
ν_2	0.238	0.484	0.691	0.605

6. Conclusion

/506

(1) Methods for measuring elastic constants of F/W cylinders as orthotropic plates were discussed. The relations between winding patterns and elastic constants were obtained in regard to F/W cylinders having both spiral and circumferential windings.

(2) The apparent values disregarding ν_1 and ν_2 differ considerably from the values of Young's moduli.

(3) The possible upper limit of Young's moduli in F/W cylinders under internal pressure was discussed.

Deep appreciation is expressed to N. Takata, N. Otani, and A. Hondo who have eagerly cooperated in the experiments, and to the Nittobo Plastic Research Labs. for their cooperation in preparing F/W cylindrical specimens.

This work was supported in part by funds allotted by V/STOL Composite Research and from Organized Research "Application of FRP in Space Engineering and Aeronautics Engineering." We would like to acknowledge their help and express our gratitude.

This translation was prepared for the National Aeronautics and Space Administration by INTERNATIONAL INFORMATION INCORPORATED
under Contract NASw-1499